


[View Journal Online](#)  
[View Article Online](#)

# Structural and surface properties of polyvinylpyrrolidone and aloe vera - capped iron oxide nanoparticles: Application in the photocatalytic degradation of methylene blue

Réné Njiké <sup>1</sup>, Adrien Pamen Yepseu <sup>1</sup>, Cyrille Ghislain Fotsop <sup>2</sup>, Giscard Doungmo <sup>3</sup>,  
 Katia Nono Nchimi <sup>1,\*</sup> and Peter Teke Ndifon <sup>1,\*</sup>

<sup>1</sup> Department of Inorganic Chemistry, Faculty of Science, University of Yaoundé I, P.O. Box 812, Yaoundé, Cameroon


<sup>2</sup> Faculty of Process and Systems Engineering, Otto von Guericke University, Magdeburg, Germany

<sup>3</sup> Institute für Anorganische Chemie, Christian-Albrechts-Universität zu Kiel, Max-Eyth-Str. 2, 24118 Kiel, Germany

\* Corresponding author at: Department of Inorganic Chemistry, Faculty of Science, University of Yaoundé I, P.O. Box 812, Yaoundé, Cameroon.  
 e-mail: [katia.nchimi@yahoo.fr](mailto:katia.nchimi@yahoo.fr) (K.N. Nchimi); [pndifon@facsciences-uy1.cm](mailto:pndifon@facsciences-uy1.cm) (P.T. Ndifon).

## RESEARCH ARTICLE



 10.5155/eurjchem.16.3.233-241.2691

Received: 16 April 2025

Received in revised form: 22 June 2025

Accepted: 26 July 2025

Published online: 30 September 2025

Printed: 30 September 2025

## ABSTRACT

Iron oxide nanoparticles were synthesized by the chemical precipitation method at 25 and 80 °C using polyvinylpyrrolidone (PVP) and aloe vera/polyvinyl pyrrolidone (AP) as capping agents. FTIR bands at 1584-1455 and 522-561 cm<sup>-1</sup> confirm the formation of PVP- and AP-capped iron oxide nanoparticles. The formation of magnetite and hematite phases was confirmed by powder X-ray Diffraction patterns. The elemental composition of the synthesized particles was confirmed by EDX. SEM analysis revealed a mixed morphology of spherical and irregular-shaped particles of average crystallite sizes ranging from 9 to 58 nm, as estimated from XRD and SEM measurements. Both PVP- and AP-capped nanoparticles were used as catalysts for the photocatalytic degradation of methylene blue under ultraviolet (UV) irradiation. After 180 min of irradiation with 20 mg of photocatalyst, degradation efficiencies of 53-82% were obtained, with AP-capped nanoparticles being more efficient, suggesting their potential as effective materials for the photocatalytic degradation of toxic dyes in wastewater.

## KEYWORDS

Aloe vera  
 Iron oxide  
 Photocatalyst  
 Surface properties  
 Polyvinyl pyrrolidone  
 Degradation of methylene blue

Cite this: *Eur. J. Chem.* 2025, 16(3), 233-241

Journal website: [www.eurjchem.com](http://www.eurjchem.com)

## 1. Introduction

There has been a great deal of recent interest in the design and fabrication of nanomaterials with specific morphologies and crystallite sizes due to their unique electrical, magnetic, optoelectronic, adsorptive and photocatalytic properties [1]. Metal oxide nanoparticles (MONPs) are versatile materials with a wide range of applications that have been extensively studied due to their high stability, ease of preparation, ability to obtain desired size, shape, and porosity, as well as large surface area to allow functionalization and interaction with biological and chemical systems [2]. Despite the effectiveness of metal oxide nanoparticles, these materials still suffer from limitations such as rapid recombination rate, wide band gap, and reusability. Among metal oxide nanoparticles, iron oxide nanoparticles (IONPs) have recently attracted considerable interest due to their biocompatibility, nontoxicity, catalytic activity, low cost, and environmental friendliness [3,4]. Iron oxide nanoparticles have been extensively studied due to their wide range of applications in biomedicine therapy, environmental remedia-

tion, catalysis, and other industrial processes due to their low band gap and magnetic properties, which makes them recyclable [4-6]. The degradation of pollutants using these materials depends on their stability and surface area. Several synthetic approaches, including physical [5-7] and chemical [8,9] methods, have been used to prepare iron oxide nanoparticles for the removal of dyes from wastewater. Dasgupta *et al.* synthesized iron (Fe<sup>2+</sup>/Fe<sup>3+</sup>) oxide nanoparticles using the chemical precipitation method and evaluated the photocatalytic activity of the particles obtained in the degradation of methylene blue (MB) [10]. Bachir *et al.* also reported the synthesis of α-Fe<sub>2</sub>O<sub>3</sub> attached to a polyurethane polymer for photocatalytic degradation of MB dye [11]. Louisah *et al.* [12] synthesized Fe<sub>3</sub>O<sub>4</sub> and studied its photocatalytic degradation of MB in water, sometimes using toxic solvents, high pressures, and temperatures and producing agglomerated iron oxide nanoparticles with various morphologies [13-15].

Co-precipitation is a wet chemical synthesis method that is easy to implement, cost-effective, and produces small nanoparticles [16]. This method uses synthetic polymers such

as polyvinylpyrrolidone (PVP) and polyvinyl alcohol (PVA) as capping agents for the preparation of iron oxide nanoparticles. Shaik *et al.* [17] synthesized iron oxide nanoparticles for hyperthermia using PVP as a sealing agent, resulting in nanoparticles with an average size of 5-9 nm, but very little attention has been given to studying their photocatalytic properties. Although efforts have been made to control the size, morphology, and dispersibility of iron oxide nanoparticles for specific applications, the subject remains a challenge due to the high magnetism of iron oxide nanoparticles, which favors agglomeration and limits their photocatalytic application [8,18].

Plant extracts such as aloe vera extract have been used for the synthesis of IONPs. These extracts which are usually made up of phytochemicals such as flavonoids, alkaloids, and polysaccharides are rich in hydroxyl and carbonyl groups that can act as reducing agents, stabilizing and capping agents, producing small, well-dispersed, and stable IONPs that can easily be used for the degradation of organic dyes [19-22].

Organic pollutants have considerable adverse effects on the environment and human health. Among the various organic pollutants, dyes are the most frequently used and are discharged into aqueous environments [20]. These dyes are dangerous, carcinogenic, and toxic and have harmful effects on human health, the environment, and aquatic ecosystems. Several methods have been used to eliminate these dyes from water sources [10,20]. Most of these methods are associated with secondary pollution problems and complicated procedures; high costs, expensive installation, incessant energy input, low disposal efficiency, and the products cannot be reused. Therefore, it is necessary to develop an efficient and environmentally friendly protocol for the degradation of toxic dyes. The degradation of Methylene blue involves the interaction of a photocatalyst (nanoparticles) with light radiation to generate reactive species (hydroxyl radicals ( $\bullet\text{OH}$ )) that break down the dye into smaller, less harmful compounds like  $\text{CO}_2$ ,  $\text{H}_2\text{O}$ , and inorganic ions. This process decolorizes and degrades methylene blue in aqueous solutions, making it a potential method for wastewater treatment. The degradation leads to the breakdown of the dye molecule, especially the aromatic rings of MB.

Several studies have been reported on the effect of polymers such as PVP or plant extracts such as aloe vera extract on the shape and size of IONPs [23], but, to our knowledge, no studies have been carried out to examine the synergistic effect of encapsulating polymers/plant extracts such as aloe vera on the size, shape, crystallinity, optical and photocatalytic properties of IONPs.

In this work, we report the synthesis of recyclable iron oxide nanoparticles using the Co-precipitation method, and we study the synergistic effect of the combination of aloe Vera gel extract and PVP as stabilizing agents on the size, morphology, crystallinity, surface properties, and agglomeration pattern of iron oxide nanoparticles. We also report the effect of temperature on the photocatalytic properties of iron oxide nanoparticles prepared using aloe Vera/PVP as a coating agent.

## 2. Experimental

### 2.1. Reagents

All reagents used in this study (Iron(III) chloride, 97%; iron(II) chloride, 43%; sodium hydroxide, 97%; ethanol, 95% and polyvinyl pyrrolidone, 100%) were obtained from commercial sources and used without further purification.

### 2.2. Instrumentation

Fourier transform infrared (FTIR) spectroscopy was performed on a Genesis FTIRTM spectrometer (ATI Mattson)

equipped with a DTGS (deuterated triglycine sulfate) detector operating in transmission mode in the spectral range of 400 to 4000  $\text{cm}^{-1}$ . X-ray diffraction (XRD) measurements were performed using a Rigaku Rint 200 diffractometer with  $\text{MoK}\alpha$  radiation source (with  $\lambda = 0.70930 \text{ nm}$ ). Scanning electron microscopy (SEM) analyses were performed using a ZEISS EVO scanning electron microscope equipped with energy-dispersive X-ray spectroscopy-EDX (Carl Zeiss Gemini SEM 500, Germany). Optical absorption measurements were conducted using an Ocean Insight FX-VIS-IRS-ES spectrophotometer at room temperature. For  $\text{N}_2$  sorption measurements, a BELSorp Max instrument was used. Before measurements, the samples were activated for 16-24 h at 100 °C under reduced pressure ( $< 10^{-2} \text{ kPa}$ ).

### 2.3. Methodology

#### 2.3.1. Preparation of aloe vera extract (AG)

Fresh aloe vera leaves were obtained from the Mfoundi market in Yaoundé and washed thoroughly with distilled water before cutting into small pieces. The whitish gel of Aloe Vera was then separated from the green part using a scalpel and macerated to obtain a liquid gel that was stored at 4 °C [23].

#### 2.3.2. Synthesis of PVP-capped iron oxide nanoparticles (IONPs)

A solution of  $\text{Fe(III): Fe(II)}$  in a 2:1 molar ratio was prepared by dissolving  $\text{FeCl}_2 \cdot 4\text{H}_2\text{O}$  and  $\text{FeCl}_3 \cdot 6\text{H}_2\text{O}$  in 30 mL of distilled water. The solution was then added dropwise to a 30 mL solution of PVP. The resulting mixture was stirred for one hour at 25 °C (room temperature) and the pH was adjusted to pH = 12 by adding NaOH (5M). The resulting mixture was stirred under  $\text{N}_2$  gas for one hour and the resulting black precipitate was washed with distilled water, centrifuged at 1000rpm and dried in an oven [24]. This precipitate was then calcined at 500°C for 2 hours to obtain the iron oxide nanoparticles. The same procedure was repeated at 80 °C. The resulting nanoparticles were labelled IP-25 and IP-80 for the sample synthesized at 25 and 80°C, respectively.

#### 2.3.3. Synthesis of AG/PVP(AP)-capped IONPs

A solution of  $\text{Fe(III): Fe(II)}$  in a molar ratio of 2:1 was prepared by dissolving  $\text{FeCl}_2 \cdot 4\text{H}_2\text{O}$  and  $\text{FeCl}_3 \cdot 6\text{H}_2\text{O}$  in 30 mL of distilled water. The solution was then added dropwise to 60 mL of a freshly prepared extract of aloe vera gel solution to which 0.2 g PVP had previously been added. The mixture was stirred for one hour at room temperature and the pH of the solution adjusted to 12 by adding NaOH (5 M). The resulting mixture was then stirred under  $\text{N}_2$  gas for one hour and the black precipitate obtained was washed, centrifuged, and dried in an oven at 60 °C for 48 hours. The precipitate obtained was then calcined at 500 °C for 2 hours to obtain iron oxide nanoparticles. The same procedure was repeated at 80 °C. The resulting nanoparticles were labelled IAP-25 and IAP-80 for the sample synthesized at 25 and 80 °C, respectively.

#### 2.3.4. Photocatalytic studies

For each photocatalytic study, 20 mg of nanoparticles as catalyst was added to a solution of methylene blue (MB), (50 mL,  $1 \times 10^{-5} \text{ mol/L}$ ) as model pollutant while stirring. The adsorption-desorption equilibrium between the nanoparticles and the MB dye solution was established for 90 min in the dark. Once equilibrium was reached, the solution was irradiated with a UV lamp of power 60  $\text{W/m}^2$  and  $\lambda = 365 \text{ nm}$ . Aliquots were collected at 15 min intervals and centrifuged.

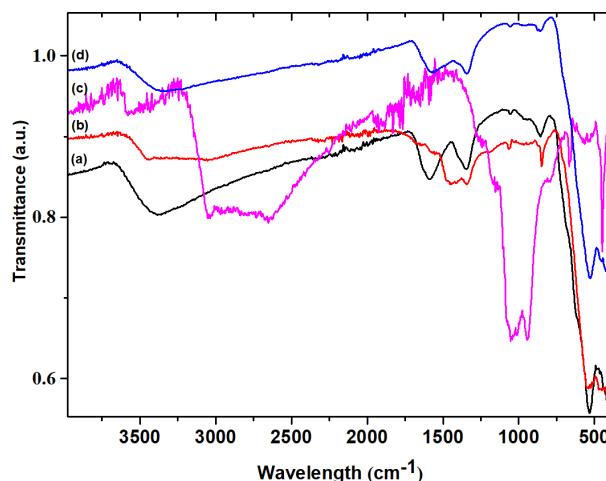


Figure 1. IR spectra of (a) IP-25, (b) IP-80, (c) IAP-80, and (d) IAP-25.

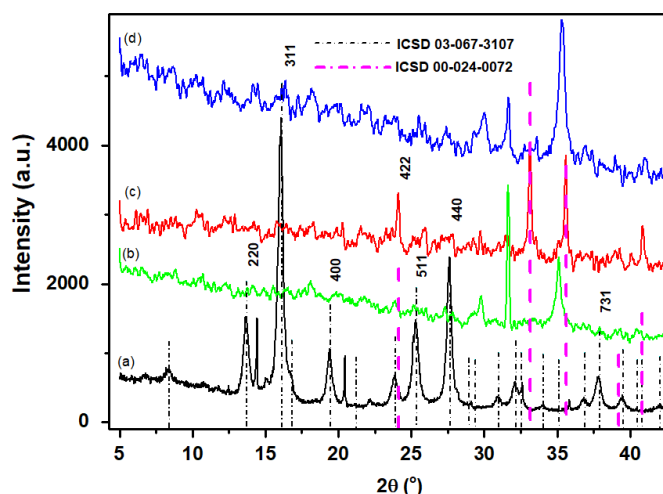


Figure 2. XRD spectra of (a) IP-25, (b) IAP-25, (c) IAP-80, and (d) IP-80.

The absorbance of the resulting solutions was analyzed using UV-Vis-NIR spectrophotometer at the maximum wavelength for MB ( $\lambda = 662$  nm). The efficiency of photodegradation for each time period was calculated using Equation 1 [25]

$$\% \text{Removal} = \frac{A_t - A_0}{A_0} \times 100 \quad (1)$$

where  $A_t$  = absorbance of MB at  $t$  seconds;  $A_0$  = initial absorbance of MB.

### 3. Results and discussions

#### 3.1. FT-IR studies

The IR spectra of iron oxide nanoparticles (IONPs) are shown in Figure 1 and the IR spectra of PVP and aloe vera are shown respectively in Figures S1a and S1b. All samples show the same peak as seen in the spectra. The bands in the range 3362-3458 and 1584-1455  $\text{cm}^{-1}$  correspond to the O-H stretching and H-O bending of adsorbed water on the surface of IAP-25, IP-25, IAP-80 and IP-80, respectively, and can be explained by the presence of PVP in the synthetic media and the probable adsorption of moisture from the atmosphere onto the surface of nanoparticles. The bands at 536, 522, 561 and 549

$\text{cm}^{-1}$  correspond to the Fe-O bond in IAP-25, IP-25, IAP-80 and IP-80, respectively [9,13,24,26,27].

#### 3.2. Powder XRD studies of PVP-capped iron oxide nanoparticles (IP-25 and IP-80)

Powder X-ray diffraction was performed on PVP-capped IONPs (IP-25 and IP-80) and aloe vera/PVP-capped IONPs (IAP-25 and IAP-80) to determine the phase composition and crystallinity. The results of the p-XRD measurements are shown in Figure 2. For IP-25, peaks were observed at  $2\theta = 13.6, 16.0, 19.4, 23.8, 25.3, 27.6, 37.8^\circ$  corresponding to the (220), (311), (400), (422), (511), (440), (731) cubic planes of magnetite phase with reference code ICSD 03-067-3107[9]. For IP-80, peaks were observed at  $2\theta = 24.0, 33.2, \text{ and } 35.5^\circ$  corresponding to the (012), (104), (110) cubic planes of the hematite phase (ICSD 00-024-0072). For IAP-25, peaks were observed at  $2\theta = 31.7, 35.3 \text{ and } 42.9^\circ$  corresponding to the (220), (311), and (400) cubic planes, corresponding to magnetite phase with reference code ICSD 03-067-3107, while for IAP-80, peaks were observed at  $2\theta = 31.7, 35.0, 45.4, 56.4^\circ$ , corresponding to (220), (311), (331), (511) cubic planes of magnetite with reference code ICSD 03-067-3107.

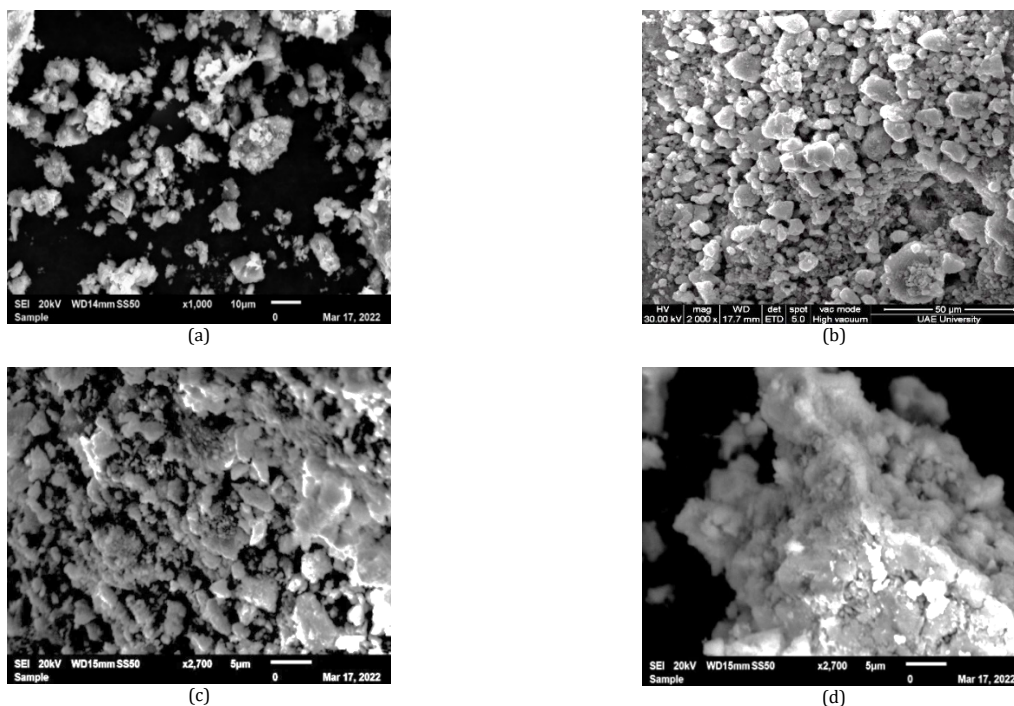


Figure 3. SEM images of (a) IP-25, (b) IP-80, (c) IAP-80, and (d) IAP-25.

The data obtained were compared with the reference data in the ICSD database, and the peaks in IP-25, IAP-25, and IAP-80 correspond exactly to the cubic phase of magnetite (ICSD 03-067-3107) while the peaks in IP-80 correspond to the cubic phase of hematite (ICSD 00-024-0072). The sizes of the nanoparticles were determined using Scherrer Equation 2:

$$D = \frac{K\lambda}{\beta \cos \theta} \quad (2)$$

$\beta$  = Full width at half maximum for the most intense diffraction peak,  $\theta$  = Angle for the most intense peak.

The crystallite sizes of IP-25 and IP-80 were determined to be 19.05 nm, and 17.26 nm, respectively. The sizes obtained in this study are smaller than those obtained by G. Pandey *et al.* [28] who synthesized magnetite with PVP as capping and obtained a crystallite size of 32 nm. On the other hand, the sizes of IAP-25 and IAP-80 were determined to be 15.28 and 57.52 nm, respectively. These results differ from those obtained in studies using aloe vera or PVP [23,29,30].

Comparing the sizes of PVP-capped IONPs and AP-capped IONPs at both temperatures, we observe that the mixed capping of IONPs with aloe vera and PVP leads to a reduction in crystallite size at low temperature (from 19.05 to 15.28 nm). Thus, we can say that the synergy between aloe vera/PVP affects the crystallite size of the particles, resulting in smaller particles than those of PVP-capped IONPs. This result obtained is comparable to that obtained by Raghad Zein *et al.* (2022) [31] who studied the influence of PVP on the properties of green synthesized silver nanoparticles. This size reduction can be explained by the synergistic action of phytochemicals in aloe vera (alkaloids, flavonoids and polysaccharides) and the C=O bond in PVP through which PVP bonds to the surface of iron oxide particles, thereby limiting particle growth [10,13,19,32]. The sizes obtained in this study are smaller than those obtained using aloe vera or PVP alone [23,33]. Thus, aloe vera/PVP can be used to synthesize IONPs of small crystallite sizes for photocatalytic applications.

### 3.3. SEM/EDX analysis

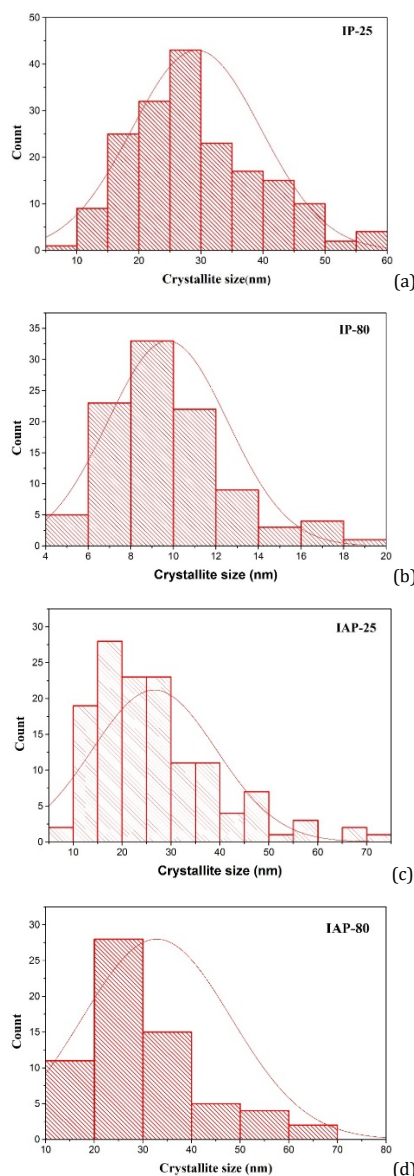
The morphology and elemental composition of the particles were determined by SEM and EDX analysis. Images of the synthesized samples are presented in Figure 3. The images show that all samples have a mixed morphology of spherical and irregularly shaped particles. The particles are more agglomerated when aloe vera/PVP is used as the capping agent than when PVP alone was used at both temperatures. This is an indication that the particles may be more dispersed in PVP than in aloe vera/PVP. Thus, the use of a combination of aloe vera/PVP as the capping agent did not improve the dispersibility of the iron oxide NPs. Furthermore, the grain size of the particles at low temperature was estimated to be  $29.2 \pm 10.4$  nm for IP-25 and  $26.5 \pm 12.7$  nm for IAP-25, while at high temperature, the grain size was estimated to be  $9.73 \pm 2.80$  nm for IP-80 and  $32.84 \pm 15.19$  nm and IAP-80, respectively [18,34].

These results suggest that the synergy between aloe vera and PVP reduces the size of the resulting particles at low temperature while favoring growth and size increase at high temperature. This increase in size can be explained by the denaturation of aloe vera with increasing temperature. Heurta *et al.* [35] showed that at 53.2 °C, 50% of the aloe vera plant membrane is damaged. This suggests that at 80 °C, the phytochemicals (flavonoids, alkaloids, and polysaccharides) in aloe vera that play an active role in the capping of the nanoparticles are structurally modified; hence, crystallite growth is preferred. The sizes obtained from SEM measurements differ from the results obtained from XRD measurements, most probably due to the agglomeration of the isolated nanoparticles. From these results, we observe that the mixing of aloe vera/PVP favors reduction in size of the resultant particles at low temperature. The particle size distribution obtained from the SEM images using ImageJ software is shown in Figure 4. Table 1 gives a summary of the crystallite sizes and grain sizes obtained in this study.



**Table 1.** Crystallite size and grain size of IONPs.

Samples	Size from SEM (nm) (Present work)	Size from XRD (nm) (Present work)	Size (nm) (Published work)
IP-25	29.20	19.05	30.00 [28]
IP-80	9.73	17.26	18.02 [30]
IAP-25	26.50	15.28	13.00 [31]
IAP-80	32.84	57.52	-

**Figure 4.** Particle size distribution of (a) IP-25, (b) IP-80, (c) IAP-8, and (d) IAP-25

The EDX spectra (Figure S2) of the different samples indicate the presence of the main elemental components of the iron oxide nanoparticles (iron (Fe), oxygen (O)) confirming the formation of the iron oxide nanoparticles. Table 2 shows a summary of the weight percentage of iron and oxygen in the different samples. The presence of Cl and Na on the EDX spectra originates from the precursors of the synthesis (Table 2).

### 3.4. Adsorption studies

The surface properties of the synthesized iron oxide nanoparticles were determined by using BET analysis for the specific surface area (S), pore diameter (Dp), and pore volume (V). The PVP-capped samples had specific surface areas of 28.98 m<sup>2</sup>g<sup>-1</sup> and 20.99 m<sup>2</sup>g<sup>-1</sup> for IP-25 and IP-80, respectively (Table

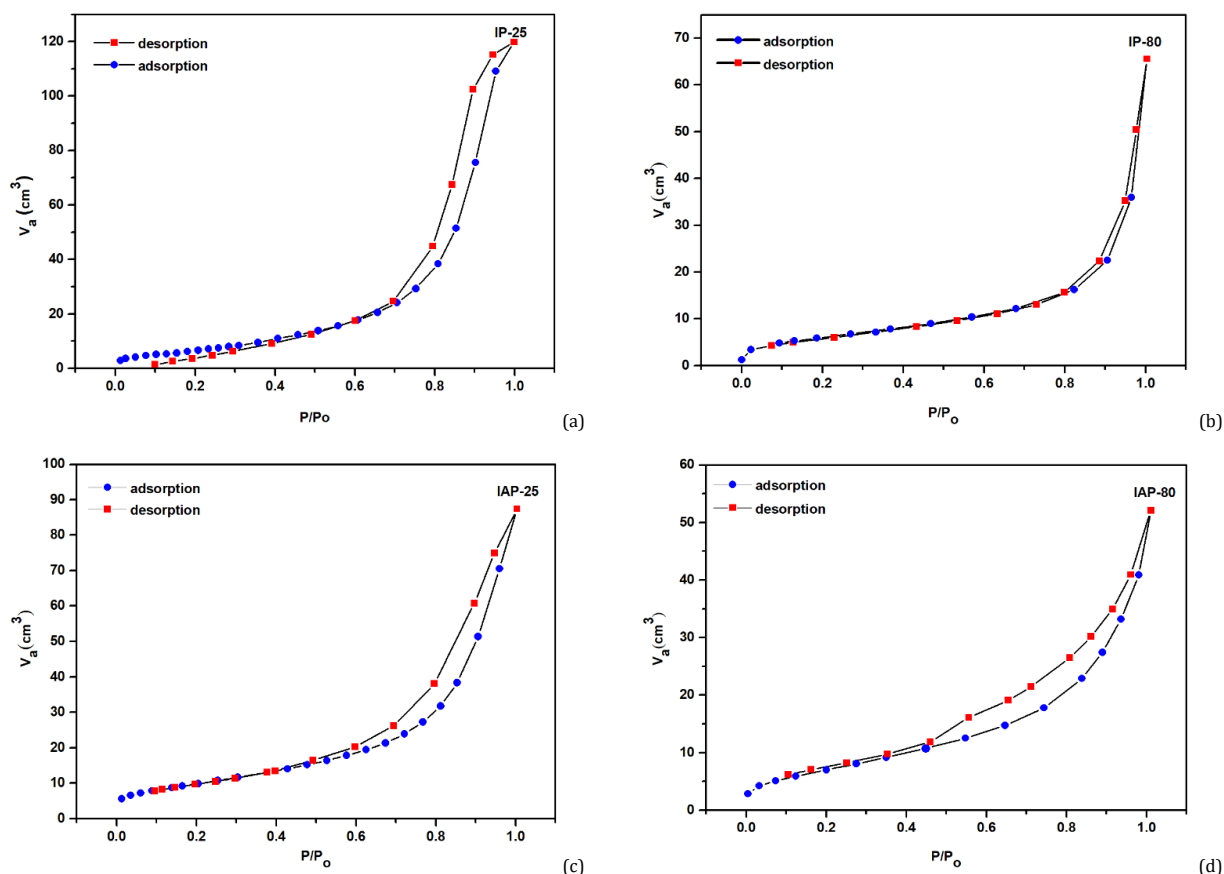
3). The aloe vera/PVP-capped samples had specific surface areas of 35.60 and 25.87 m<sup>2</sup>g<sup>-1</sup> for IAP-25 and IAP-80, respectively (Table 3). The results show that the dual capping of aloe vera and PVP increases the surface area of the synthesized IONPs. Porous volumes were evaluated as 0.021, 0.014, 0.024 and 0.018 cm<sup>3</sup>g<sup>-1</sup> for IP-25, IP-80, IAP-25, and IAP-80 respectively. The mean pore diameters were evaluated as 2.89, 2.70, 2.73, 2.78 nm for IP-25, IP-80, IAP-25 and IAP-80, respectively. The results indicate that all materials are mesoporous [12] and can be used effectively as adsorbents and for photocatalytic applications. Table 3 summarizes the BET results.

**Table 2.** Weight percentages of Fe and O

Sample	Fe	O
IO-PVP-25	41.60	21.90
IO-PVP-80	65.60	23.10
IO-AP-25	50.80	22.20
IO-AP-80	39.00	31.60

**Table 3.** Surface characteristics of iron oxide nanoparticles.

Samples	Specific surface area ( $S/m^2g^{-1}$ )	Pore diameter ( $D_p/nm$ )	Pore volume ( $V/cm^3g^{-1}$ )
IP-25	28.98	2.89	0.021
IP-80	20.99	2.70	0.014
IAP-25	35.60	2.73	0.024
IAP-80	25.87	2.78	0.018

**Figure 5.** Adsorption-desorption isotherms for (a) IP-25, (b) IP-80, (c) IAP-25, and (d) IAP-80.

The adsorption isotherms (Figure 5) of both IP-25 and IP-80 are more likely to follow the type IV adsorption isotherm and hysteresis loop of type H4, as obtained by Pandey *et al.* [28]. However, the IONPs capped with aloe vera/PVP are likely to follow the type IV adsorption isotherm with hysteresis loop H3 [36]. This suggests a change in the shape of pores from small slit-shapes to larger slit shapes, increasing the surface area available for light interaction [37]. Therefore, this study shows that the dual capping of aloe vera/polyvinylpyrrolidone (PVP) enhances the surface area and modifies the shape of the pores of IONPs, making them favorable for use in photocatalysis.

### 3.5. Optical properties of IONPs

The optical properties of the IONPs were studied by measuring their UV absorbance (Figure S3-S6). The energy band gaps of the IONPs were determined from the Tauc plots (Figure S7). The energy band gap of 2.40 eV and 1.60 eV was obtained for IP-25 and IP-80, respectively, similar to those reported from previous studies [23,33]. The energy band gaps for IAP-25 and IAP-80 were found to be 2.60 eV and 2.20 eV, respectively. This

result indicates that mixing aloe vera and PVP causes a blue shift in the energy band gaps of PVP-capped IONPs. This observed increase in the energy band gap could be due to the reduction in the nanometric size of the nanoparticles, which clearly shows the effect of the addition of aloe vera on the optical properties of the nanoparticles [38].

### 3.6. Photocatalytic studies

The photocatalytic properties of the synthesized IONPs were examined by photocatalytic degradation of the MB dye using these materials as photocatalysts. Figure S8 shows the photocatalytic activity of each sample over a 180-minute period. MB was used as a dye to investigate the photocatalytic properties of the synthesized nanoparticles. The initial absorbance of MB ( $A_0$ ) was taken and the absorbance ( $A_t$ ) was monitored at 15 minute intervals for 180 minutes. The absorbances were recorded at a maximum wavelength of 662 nm. The degradation efficiency of the MB dye was calculated for each prepared sample over the 180-minute period as shown in Figure 6.

**Table 4.** Comparison of MB dye degradation with iron oxides.

Dye	Source of light and intensity	Time of irradiation/mins	pH	% Degradation	Reference
MB	UV lamp, 150W	60	7	25	[12]
MB	Sunlight	120	7	34	[42]
MB	Mercury UV lamp, 250 W	90	7	45	[43]
MB	Xenon, Visible light	360	7	60	[41]
Rhodamine B	Sunlight	60	-	24	[44]
MB	UV lamp, 60W	120	7	81	Present work

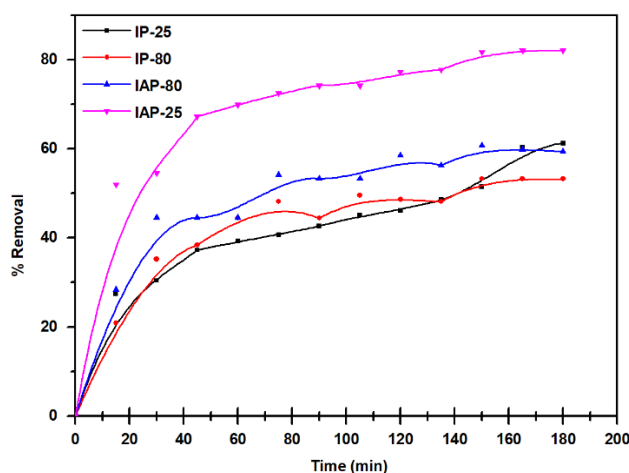
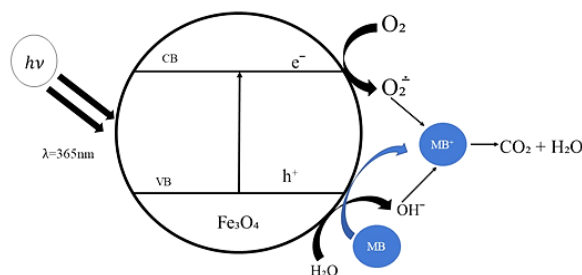
**Figure 6.** Photodegradation efficiency of IP-25, IP-80, IAP-25, and IAP-80.**Figure 7.** Mechanism and schematic diagram of the photodegradation of MB by IONPs.

Figure 6 shows that all IONPs synthesized have some photo-catalytic activity. PVP-capped samples have photocatalytic activity lower than that of the synergistically synthesized aloe vera/PVP-capped IONPs. This suggests that the dual capping of aloe vera/PVP enhances the photocatalytic activity of IONPs. This increase in photocatalytic activity can be attributed to the larger surface area of aloe vera/PVP-capped IONPs resulting from a change in the pore shape from small to large slits. The larger slit pores allow for greater adsorption of MB dye before degradation by photoexcited electrons [39]. The study achieved a degradation efficiency of 81 % at pH = 7 using the IAP-25 sample, which is higher than the 25 % achieved by Louisah *et al.* [12] who used iron oxide nanoparticles synthesized with Burkeana plant extract for photocatalytic degradation of MB at pH = 7. The proposed mechanism of degradation of MB by  $\text{Fe}_3\text{O}_4$  is as follows [40,41].

UV light strikes bare  $\text{Fe}_3\text{O}_4$  inducing the photogeneration electrons and holes.



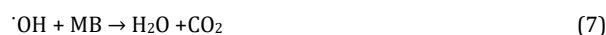
The photogenerated electrons are picked up by dissolved oxygen ( $\text{O}_2$ ) in water to produce an active radical specie ( $\text{O}_2^{\cdot-}$ ).



Photogenerated holes ( $h^+$ ) are picked up by water molecules ( $\text{H}_2\text{O}$ ) to form OH.



Free radicals ( $\text{O}_2^{\cdot-}$  and  $\cdot\text{OH}$ ) are responsible for the degradation of activated MB.



The schematic diagram presented in Figure 7 illustrates the degradation mechanism of MB on IONP photocatalysts. The degradation efficiencies obtained in this study were compared with those of similar studies in the literature (Table 4) and the results show that the catalysts obtained in this study have improved the degradation efficiencies of the dye.

#### 4. Conclusions

IONPs were successfully synthesised using only PVP only and combined aloe vera/PVP as capping agents. The aloe vera/PVP-capped IONPs exhibited smaller crystallite sizes as the PVP-capped IONPs, indicating that this method of synthesis is effective in producing small-sized IONPs. An increase in the synthesis temperature favoured the growth of crystallites in the

aloe vera/PVP-capped IONPs. The synthesis approach using combined capping agents (aloe vera/PVP) has a synergistic effect on the size of the IONPs, reducing crystallite growth and hence increasing the surface area of the IONPs, suggesting its potential use to synthesize IONPs with favorable surface properties for photocatalytic degradation of dyes like methylene blue. IONPs capped with aloe vera/PVP and synthesized at low temperatures exhibit a higher photocatalytic degradation efficiency, indicating that high temperature has an impact on the photocatalytic degradation efficiency of IONPs on MB using aloe vera/PVP.

## Acknowledgements

We thank the Alexander von Humboldt Foundation for a postdoctoral fellowship to (KNN). The authors also acknowledge the final assistance through the 'Fond de modernization et d'appui à la recherche' allocation to Higher Education Teachers of Cameroon (KNN and PTN).

## Supporting information

The data used to support the findings of this study are included in the article. Any other data are available from the corresponding author upon request. Electronic supplementary information (ESI) available: IR spectra of capping agents, UV spectra of nanoparticles, and photodegradation curves.

## Disclosure statement

Conflict of interest: The authors declare that they have no conflict of interest. Sample availability: Samples of the compounds are available from the author.

## CRediT authorship contribution statement

Conceptualization: Katia Nono Nchimi, Peter Teke Ndifon; Methodology: René Njiké, Adrien Pamen Yepseu; Giscard Doungmo; Validation: Katia Nono Nchimi; Formal Analysis: René Njiké, Adrien Pamen Yepseu; Giscard Doungmo; Investigation: René Njiké, Cyrille Ghislain Fotsop; Resources: Katia Nono Nchimi, Peter Teke Ndifon; Data Curation: Adrien Pamen Yepseu, Cyrille Ghislain Fotsop; Writing - Original Draft: René Njiké, Adrien Pamen Yepseu; Writing - Review and Editing: Katia Nono Nchimi, Peter Teke Ndifon; Visualization: Katia Nono Nchimi; Funding acquisition: Katia Nono Nchimi, Peter Teke Ndifon; Supervision: Katia Nono Nchimi, Peter Teke Ndifon; Project Administration: Peter Teke Ndifon.

## ORCID and Email

René Njiké

 [rene.njike@facsciences-uy1.cm](mailto:rene.njike@facsciences-uy1.cm)

 <https://orcid.org/0009-0000-9670-830X>

Adrien Pamen Yepseu

 [yepseuadrien@gmail.com](mailto:yepseuadrien@gmail.com)


 <https://orcid.org/0000-0002-2773-1351>

Cyrille Ghislain Fotsop

 [fotsopcyril@yahoo.fr](mailto:fotsopcyril@yahoo.fr)

 <https://orcid.org/0000-0001-6455-2515>

Giscard Doungmo

 [gdoungmo@ac.uni-kiel.de](mailto:gdoungmo@ac.uni-kiel.de)

 <https://orcid.org/0000-0002-6332-8260>

Katia Nono Nchimi

 [katia.nchimi@yahoo.fr](mailto:katia.nchimi@yahoo.fr)

 <https://orcid.org/0000-0002-5031-6404>

Peter Teke Ndifon

 [pndifon@facsciences-uy1.cm](mailto:pndifon@facsciences-uy1.cm)

 <https://orcid.org/0000-0001-9331-9034>

## References

- [1]. Herlekar, M.; Barve, S.; Kumar, R. Plant-Mediated Green Synthesis of Iron Nanoparticles. *J. Nanoparticles* **2014**, *2014*, 1–9.
- [2]. Sanchez-Moreno, P.; Ortega-Vinuesa, J. L.; Paula-Garcia, J. M.; Marchal, J. A.; Boulaiz, H. Smart Drug-Delivery Systems for Cancer Nanotherapy. *CDT*. **2018**, *19* (4), 339–359.
- [3]. Jana, T. K.; Pal, A.; Mandal, A. K.; Sarwar, S.; Chakrabarti, P.; Chatterjee, K. Photocatalytic and antibacterial performance of  $\alpha$ -Fe<sub>2</sub>O<sub>3</sub> nanostructures. *ChemistrySelect* **2017**, *2*, 3068–3077.
- [4]. Machala, L.; Zboril, R.; Gedanken, A. Amorphous Iron(III) Oxide — A Review. *ChemInform*. **2007**, *38* (28), 4003–4018 <https://doi.org/10.1002/chin.200728192>.
- [5]. Montiel Schneider, M. G.; Martin, M. J.; Otárola, J.; Vakarelska, E.; Simeonov, V.; Lassalle, V.; Nedyalkova, M. Biomedical Applications of Iron Oxide Nanoparticles: Current Insights Progress and Perspectives. *Pharmaceutics* **2022**, *14* (1), 204.
- [6]. Tharani, K.; Jegatha Christy, A.; Sagadevan, S.; Nehru, L. Photocatalytic and antibacterial performance of iron oxide nanoparticles formed by the combustion method. *Chemical. Physics. Letters* **2021**, *771*, 138524. duplicated
- [7]. Pecharroman, C.; Gonzalez-Carreao, T.; Iglesias, J. The Infrared Dielectric Properties of Maghemite, -Fe<sub>2</sub>O<sub>3</sub>, from Reflectance Measurement on Pressed Powders. *Phys. Chem. Miner.* **1995**, *22* (1). <https://doi.org/10.1007/BF00202677>
- [8]. Criveanu, A.; Dumitrache, F.; Fleaca, C.; Gavrilă-Florescu, L.; Lungu, I.; Morjan, I. P.; Socoliuc, V.; Prodan, G. Chitosan-coated iron oxide nanoparticles obtained by laser pyrolysis. *Applied Surface Science Advances* **2023**, *15*, 100405.
- [9]. Noqta, O. A.; Aziz, A. A.; Usman, A. I. Synthesis of PVP Coated Superparamagnetic Iron Oxide Nanoparticles with a High Saturation Magnetization. *SSP*. **2019**, *290*, 301–306.
- [10]. Dasgupta, N.; Nayak, M. A.; Gauthier, M. Starch-stabilized iron oxide nanoparticles for the photocatalytic degradation of methylene blue. *Polysaccharides* **2022**, *3*, 655–670.
- [11]. Yaou Balarabe, B.; Illiassou Oumarou, M. N.; Koroney, A. S.; Adjama, I.; Ibrahim Baraze, A. R. Photo-Oxidation of Organic Dye by Fe<sub>2</sub>O<sub>3</sub> Nanoparticles: Catalyst, Electron Acceptor, and Polyurethane Membrane (PU-Fe<sub>2</sub>O<sub>3</sub>) Effects. *J. Nanotechnology* **2023**, *2023*, 1–12.
- [12]. Mahlaule-Glory, L. M.; Mapetla, S.; Makofane, A.; Mathipa, M. M.; Hintsho-Mbita, N. C. Biosynthesis of iron oxide nanoparticles for the degradation of methylene blue dye, sulfisoxazole antibiotic and removal of bacteria from real water. *Heliyon* **2022**, *8* (9), e10536.
- [13]. Silva, M. F.; de Oliveira, L. A.; Ciciliati, M. A.; Lima, M. K.; Ivashita, F. F.; Fernandes de Oliveira, D. M.; Hechenleitner, A. A.; Pineda, E. A. The Effects and Role of Polyvinylpyrrolidone on the Size and Phase Composition of Iron Oxide Nanoparticles Prepared by a Modified Sol-Gel Method. *J. Nanomaterials* **2017**, *2017*, 1–10.
- [14]. Marand, Z. R.; Rashid Farimani, M. H.; Shahtahmasebi, N. Study of magnetic and structural and optical properties of Zn doped Fe<sub>3</sub>O<sub>4</sub> nanoparticles synthesized by co-precipitation method for biomedical application. *Nanomed. J.* **2014**, *1*, 238–247. <https://doi.org/10.7508/NMJ.2015.04.004>
- [15]. Teng, Y.; Li, Y.; Li, Y.; Song, Q. Preparation of Fe<sub>3</sub>O<sub>4</sub>/PVP magnetic nanofibers via in situ method with electrospinning. *J. Phys.: Conf. Ser.* **2020**, *1549* (3), 032087.
- [16]. Fujishima, A.; Honda, K. Electrochemical Photolysis of Water at a Semiconductor Electrode. *Nature*. **1972**, *238* (5358), 37–38.
- [17]. Fu, C.; Ravindra, N. M. Magnetic iron oxide nanoparticles: synthesis and applications. *Bioinspired, Biomimetic Nanobiomaterials* **2012**, *1* (4), 229–244.
- [18]. Shaikh, I. A.; Shah, D. V. Synthesis of PVP capped superparamagnetic iron oxide (Fe<sub>3</sub>O<sub>4</sub>) nanoparticles in the inert atmosphere - An ideal candidate for hyperthermia. *AIP. Conference Proceedings* **2019**, *2162*, 020113.
- [19]. Jeevanandam, J.; Chan, Y. S.; Danquah, M. K. Biosynthesis of Metal and Metal Oxide Nanoparticles. *ChemBioEng. Reviews* **2016**, *3* (2), 55–67.
- [20]. Nagajyothi, P. C.; Prabhakar Vattikuti, S. V.; Devarayapalli, K. C.; Yoo, K.; Shim, J.; Sreekanth, T. V. Green synthesis: Photocatalytic degradation of textile dyes using metal and metal oxide nanoparticles-latest trends and advancements. *Critical Reviews Environmenta. Science and. Technology* **2019**, *50* (24), 2617–2723.
- [21]. Ali, K.; Ahmed, B.; Khan, M. S.; Musarrat, J. Differential surface contact killing of pristine and low EPS *Pseudomonas aeruginosa* with Aloe vera capped hematite ( $\alpha$ -Fe<sub>2</sub>O<sub>3</sub>) nanoparticles. *Journal of Photochemistry and Photobiology B: Biology* **2018**, *188*, 146–158.
- [22]. Phumying, S.; Labuayai, S.; Thomas, C.; Amornkitbamrung, V.; Swatsitang, E.; Maensiri, S. Aloe vera plant-extracted solution hydrothermal synthesis and magnetic properties of magnetite (Fe<sub>3</sub>O<sub>4</sub>) nanoparticles. *Appl. Phys. A* **2012**, *111* (4), 1187–1193.
- [23]. Rahmani, R.; Gharanfoli, M.; Gholamin, M.; Darroudi, M.; Chamani, J.; Sadri, K.; Hashemzadeh, A. Plant-mediated synthesis of superparamagnetic iron oxide nanoparticles (SPIONs) using aloe vera and flaxseed extracts and evaluation of their cellular toxicities. *Ceramics International* **2020**, *46* (3), 3051–3058.
- [24]. Nchimi Nono, K.; Vahl, A.; Terraschke, H. Towards High-Performance Photo-Fenton Degradation of Organic Pollutants with Magnetite-Silver Composites: Synthesis, Catalytic Reactions and in Situ Insights. *Nanomaterials (Basel)* **2024**, *14* (10), 849.
- [25]. Yepseu, A. P.; Girardet, T.; Nyamen, L. D.; Fleutot, S.; Ketchemen, K. I.; Cleymand, F.; Ndifon, P. T. Copper (II) Heterocyclic Thiosemicarbazone Complexes as Single-Source Precursors for the



- Preparation of Cu<sub>9</sub>S<sub>5</sub> Nanoparticles: Application in Photocatalytic Degradation of Methylene Blue. *Catalysts* **2022**, 12 (1), 61.
- [26]. Morales Morales, J. A. Synthesis of Hematite  $\alpha$ -Fe<sub>2</sub>O<sub>3</sub> Nano Powders by the Controlled Precipitation Method / Síntesis de Nano Polvos de Hematita  $\alpha$ -Fe<sub>2</sub>O<sub>3</sub> Por El Método de Precipitación. *Cienc. Desarro.* **2017**, 8 (1), 99–107.
- [27]. Lassoued, A.; Dkhil, B.; Gadri, A.; Ammar, S. Control of the shape and size of iron oxide ( $\alpha$ -Fe<sub>2</sub>O<sub>3</sub>) nanoparticles synthesized through the chemical precipitation method. *Results in Physics* **2017**, 7, 3007–3015.
- [28]. Pandey, G.; Singh, S.; Hitkari, G. Synthesis and characterization of polyvinyl pyrrolidone (PVP)-coated Fe<sub>3</sub>O<sub>4</sub> nanoparticles by chemical co-precipitation method and removal of Congo red dye by adsorption process. *Int. Nano. Lett.* **2018**, 8 (2), 111–121.
- [29]. Itoh, H.; Sugimoto, T. Systematic Control of Size, Shape, Structure, and Magnetic Properties of Uniform Magnetite and Maghemite Particles. *J. Colloid Interface Sci.* **2003**, 265 (2), 283–295.
- [30]. Agarwal, T.; A. Gupta, K.; Alam, S.; G. H. Zaidi, M. Fabrication and Characterization of Iron Oxide Filled Polyvinyl Pyrrolidone Nanocomposites. *Cmaterials* **2012**, 2 (3), 17–21.
- [31]. Zein, R.; Alghoraibi, I.; Soukkarieh, C.; Ismail, M. T.; Alahmad, A. Influence of Polyvinylpyrrolidone Concentration on Properties and Anti-Bacterial Activity of Green Synthesized Silver Nanoparticles. *Micromachines* **2022**, 13 (5), 777.
- [32]. Kahramanoğlu, I.; Chen, C.; Chen, J.; Wan, C. Chemical Constituents, Antimicrobial Activity, and Food Preservative Characteristics of Aloe vera Gel. *Agronomy* **2019**, 9 (12), 831.
- [33]. Mandal, B. K.; Biswas, A.; Barman, S.; Das, R.; Debnath, P. S. Structural study of iron oxide nanoparticles (INPs) synthesized in aloe vera plant extract. *AIP. Conference. Proceedings* **2020**, 2220, 020185.
- [34]. Yazid, N. A.; Joon, Y. C. Co-precipitation synthesis of magnetic nanoparticles for efficient removal of heavy metal from synthetic wastewater. *AIP. Conference. Proceedings* **2019**, <https://doi.org/10.1063/1.5117079>.
- [35]. Huerta, C.; Freire, M.; Cardemil, L. Expression of hsp70, hsp100 and ubiquitin in Aloe barbadensis Miller under direct heat stress and under temperature acclimation conditions. *Plant. Cell. Rep.* **2012**, 32 (2), 293–307.
- [36]. Sing, K. S. W.; Williams, R. T. Physisorption Hysteresis Loops and the Characterization of Nanoporous Materials. *Adsorp. Sci. Technol.* **2004**, 22 (10), 773–782.
- [37]. AlAbduljabbar, F. A.; Haider, S.; Ali, F. A.; Alghyamah, A. A.; Almasry, W. A.; Patel, R.; Mujtaba, I. M. Efficient Photocatalytic Degradation of Organic Pollutant in Wastewater by Electrospun Functionally Modified Polyacrylonitrile Nanofibers Membrane Anchoring TiO<sub>2</sub> Nanostructured. *Membranes* **2021**, 11 (10), 785.
- [38]. Deotale, A. J.; Nandedkar, R. Correlation between Particle Size, Strain and Band Gap of Iron Oxide Nanoparticles. *Materials Today: Proceedings* **2016**, 3 (6), 2069–2076.
- [39]. Kumar, A. A Review on the Factors Affecting the Photocatalytic Degradation of Hazardous Materials. *Int. J. Mater Sci. Eng. MSEIJ* **2017**, 1 (3), <https://doi.org/10.15406/mseij.2017.01.00018>.
- [40]. Ahmad, W.; Khan, A. U.; Shams, S.; Qin, L.; Yuan, Q.; Ahmad, A.; Wei, Y.; Khan, Z. U.; Ullah, S.; Rahman, A. U. Eco-benign approach to synthesize spherical iron oxide nanoparticles: A new insight in photocatalytic and biomedical applications. *Journal of Photochemistry and Photobiology. B: Biology* **2020**, 205, 111821.
- [41]. Ganeshraja, A. S.; Rajkumar, K.; Zhu, K.; Li, X.; Thirumurugan, S.; Xu, W.; Zhang, J.; Yang, M.; Anbalagan, K.; Wang, J. Facile synthesis of iron oxide coupled and doped titania nanocomposites: tuning of physicochemical and photocatalytic properties. *RSC. Adv.* **2016**, 6 (76), 72791–72802.
- [42]. Šmitran, A.; Jelić, D.; Pržulj, S.; Vračević, S.; Gajić, D.; Malinović, M.; Božić, L. Study of iron oxide nanoparticles doped with copper: antimicrobial and photocatalytic activity. *Contemp. Mater. CM.* **2020**, 11 (2), 93–101 <https://doi.org/10.7251/COMEN2002093>.
- [43]. Wu, W.; Xiao, X.; Zhang, S.; Ren, F.; Jiang, C. Facile method to synthesize magnetic iron oxides/TiO<sub>2</sub> hybrid nanoparticles and their photodegradation application of methylene blue. *Nanoscale. Res. Lett.* **2011**, 6 (1), <https://doi.org/10.1186/1556-276X-6-533>.
- [44]. Duy Vu Nguyen, K.; Dang Nguyen Vo, K. Magnetite nanoparticles-TiO<sub>2</sub> nanoparticles-graphene oxide nanocomposite: Synthesis, characterization and photocatalytic degradation for Rhodamine-B dye. *AIMS. Materials Science* **2020**, 7 (3), 288–301.



Copyright © 2025 by Authors. This work is published and licensed by Atlanta Publishing House LLC, Atlanta, GA, USA. The full terms of this license are available at <https://www.eurjchem.com/index.php/eurjchem/terms> and incorporate the Creative Commons Attribution-Non Commercial (CC BY NC) (International, v4.0) License (<http://creativecommons.org/licenses/by-nc/4.0>). By accessing the work, you hereby accept the Terms. This is an open access article distributed under the terms and conditions of the CC BY NC License, which permits unrestricted non-commercial use, distribution, and reproduction in any medium, provided the original work is properly cited without any further permission from Atlanta Publishing House LLC (European Journal of Chemistry). No use, distribution, or reproduction is permitted which does not comply with these terms. Permissions for commercial use of this work beyond the scope of the License (<https://www.eurjchem.com/index.php/eurjchem/terms>) are administered by Atlanta Publishing House LLC (European Journal of Chemistry).